Quantum dynamics in a single excitation subspace: deviations from eigenstate thermalization via long time correlations

OPEN ACCESS
IOP Publishing
Journal of Physics A: Mathematical and Theoretical
J. Phys. A: Math. Theor. **55** (2022) 475303 (25pp)
https://doi.org/10.1088/1751-8121/aca3dc

Quantum dynamics in a single excitation subspace: deviations from eigenstate thermalization via long time correlations

Charlie Nation[1,2,*] **and Diego Porras**[3]

[1] Department of Physics and Astronomy, University College London, London WC1E 6BT, United Kingdom
[2] Department of Physics and Astronomy, University of Sussex, Brighton BN1 9QH, United Kingdom
[3] Institute of Fundamental Physics, IFF-CSIC, Calle Serrano 113B, 28006 Madrid, Spain

E-mail: C.Nation@sussex.ac.uk

Received 30 March 2022; revised 18 October 2022
Accepted for publication 17 November 2022
Published 5 December 2022

Abstract

In this work we study a scenario where unitary quantum dynamics in a many-body interacting system is restricted to a single excitation subspace. We ask how dynamics within to such a subspace may in general differ from predictions of the eigenstate thermalization hypothesis (ETH). We show that for certain initial states and observables, if thermalization occurs, it will not fulfil other key predictions of the ETH; instead following differing generic behaviours. We show this by analysing long-time fluctuations, two-point correlation functions, and the out-of-time-ordered correlator; analytically detailing deviation from ETH predictions. We derive instead an ETH-like relation, with non-random off-diagonals for matrix elements of observables, with correlations which alter long-time behaviour and constrain dynamics. Further, we analytically compute the time-dependence of the decay to equilibrium, showing it is proportional to the survival probability of the initial state. We finally note the conditions studied are common in many physical scenarios, such as under the rotating-wave

* Author to whom any correspondence should be addressed.

approximation. We show numerically our predictions are robust to perturbations which break this approximation.

Keywords: thermalization, ergodicity, quantum information scrambling, integrability

(Some figures may appear in colour only in the online journal)

1. Introduction

The thermalization of closed quantum systems has seen a large amount of interest in recent years [1–8], inspired by the modern experimental capability to observe their unitary evolution in the laboratory [9–15]. For non-integrable systems, the eigenstate thermalization hypothesis (ETH) is understood to be the key physical mechanism behind thermalization [1, 4, 16–20]. The ETH can be written as a condition for the matrix elements of observables of a quantum many-body system. This conjecture can be motivated from random matrix theory (RMT) by assuming a non-integrable quantum Hamiltonian can be expressed as a perturbation of a non-interacting or integrable model. As shown by Deutsch [16], this random matrix approach can be used to prove that time-averages of a typical observable are equivalent to microcanonical averages, which is one of the conditions required for a quantum system to thermalize. Deutsch's approach has been applied and extended significantly in recent years to treat a larger class of Hamiltonians, as well as time-dependence and fluctuations of observables [21–25]. The second requirement for quantum thermalization is exponentially decreasing observable fluctuations with system size. This is also guaranteed by the ETH in the form of Srednicki's ansatz [17, 26].

The ETH implies that generic closed chaotic quantum systems display many universal behaviours, independent of any particular form of the Hamiltonian. These universal behaviours are closely linked with the behaviours of random matrix models [16, 22–24, 27]. One may expect the presence of conservation laws may cause deviations from quantum chaos as described by RMT, with the most obvious example being integrable systems, with an extensive number of conserved quantities [28]; what is not obvious is the possible effect of one, or a few, conservation laws on the route to equilibrium and other markers of thermalization.

We will see for given realistic initial states and observables a single conserved quantity has a profound effect on dynamics, causing a departure from the expected behaviours implied by the ETH, *even in the case of non-integrable systems*. We study this departure in three key ways: (a) fluctuations from equilibrium, (b) behaviour of two-time correlation functions, (c) scrambling of quantum information as measured via the out-of-time ordered correlator (OTOC). We further study the time-dependence of observables after a quantum quench—a topic which has seen significant recent interest [23, 24, 29–33]. We obtain an explicit form for the time-dependence in terms of the survival probability of the initial state.

The introduction of symmetries in order to avoid thermalization is a topic which has been previously considered [34], and somewhat controversial, where the ETH can be seen to still hold in each symmetry sector [35]. Similarly, non-thermal subspaces may be engineered in the form of quantum many-body scars [36, 37]; first experimentally observed in non-thermal behaviour in Rydberg atoms [38] for particular initial states. The deviation from ETH predictions in systems exhibiting quantum many-body scars is often closely related to a symmetry of some Hamiltonian H_0. For example, one may perturb the Hamiltonian in such a way that this symmetry is now a dynamical symmetry [36], or spectrum generating algebra, thus yielding a set of eigenstates which exhibit non-thermal behaviour. Similar conditions may even generate

non-stable long-time dynamics in open systems [39]. In contrast, we report here a simpler example of non-thermal behaviour which manifests in the fluctuations of specific observables for particular initial states corresponding to a Hamiltonian symmetry, as well as a symmetry of some subspace. Further, in the systems we analyse thermalization *does* occur for the studied initial states. The deviation from the ETH lies solely in observable fluctuations and time correlations. We stress our claim is not that the system studied violates the ETH for bulk mid-energy eigenstates in each symmetry sector—indeed, for the vast majority of physically relevant initial states and observables we observe behaviour expected from the ETH.

We further note that the OTOC has been previously understood as a witness of quantum phase transitions: in [40] the long-time value of the OTOC was seen to probe quantum phase transitions in non-integrable quantum spin chain system. Here the authors observe in one phase the OTOC is approximately described by its ground state contribution at long times, as contributions by excited states are suppressed. Indeed, in the following we observe a phenomenologically similar mechanism, where contributions to the long-time OTOC are suppressed by the choice of observable and initial state.

This article is arranged as follows. First, we review some generic properties of non-integrable systems implied by the ETH, that are to be studied later in the presence of conservation law. We then outline a very simple case where such generic properties can be seen to differ from the ETH prediction, giving an intuition for the main physical mechanism behind the deviation. We then apply this approach to more general observables, and show that it leads to a scaling of time fluctuations which violates the ETH prediction. We then use the same approach developed for long-time fluctuations to understand both the equilibration in time of observables, and the scrambling of quantum information. Throughout, we present exact diagonalization calculations to demonstrate our analytical arguments.

2. Properties of chaotic quantum systems

In this section we review some generic properties of non-integrable systems that are assumed to abide by the ETH. A typical scenario considered in this work, is a 'quantum quench'; whereby we initialize with some non-interacting Hamiltonian H_0, and prepare the system in and eigenstate $|\phi_{\alpha_0}\rangle$ of H_0. At $t=0$, an interaction Hamiltonian V is introduced, which renders the total Hamiltonian $H = H_0 + V$ non-integrable. The many-body Hamiltonian, H, has eigenstates and eigenvalues $|\psi_\mu\rangle$ and E_μ, respectively.

To simplify the discussion, we focus on observables O that have a diagonal structure in the basis of H_0. Initialized in a state $|\psi(0)\rangle = |\phi_{\alpha_0}\rangle = \sum_\mu c_\mu(\alpha_0)|\psi_\mu\rangle$, the initial observable expectation value $\langle O(t)\rangle = O_{\alpha_0\alpha_0}$. After the perturbation V is turned on, the system thermalizes; that is, observables evolve to an equilibrium given by the microcanonical ensemble $\langle O\rangle_{\rm MC} = \langle O\rangle_{\rm MC}(E_{\alpha_0})$, which depends only on the initial state energy.

Here and in the following we use the notation $O_{\mu\nu}$ with subscripts μ,ν to indicate matrix elements in the interacting basis of the full Hamiltonian H, $O_{\mu\nu} := \langle\psi_\mu|O|\psi_\nu\rangle$, and $O_{\alpha\beta}$ with subscripts α,β to indicate matrix elements in the non-interacting basis $O_{\alpha\beta} := \langle\phi_\alpha|O|\phi_\beta\rangle$.

The ETH is a conjecture on the properties of chaotic systems that provides a mechanism for thermalization, and can be written as an ansatz on observable matrix elements, $O_{\mu\nu}$ in the energy eigenbasis [17, 26]:

$$O_{\mu\nu} = \mathcal{O}(E)\delta_{\mu\nu} + \frac{1}{\sqrt{D(E)}} f(E,\omega)\mathcal{R}_{\mu\nu}, \tag{1}$$

where $E = \frac{E_\mu + E_\nu}{2}$, $\omega = E_\mu - E_\nu$, f and $\mathcal{O} \approx \langle O \rangle_{\mathrm{MC}}$ are smooth functions of their respective parameters. The function $f(E, \omega)$ has an energy width that determines the energy window under which two energy eigenstates have a non-negligible observable matrix element. $D(E)$ is the density of states at energy E, and $\mathcal{R}_{\mu\nu}$ is a stochastic variable of zero mean and unit variance.

Chaotic quantum systems are often characterized by an effective description in terms of RMT [6, 16, 21, 41–43]. Indeed, an RMT approach can be exploited to derive the full form of equation (1) [22], as well as the full dynamics of the decay process, and subsequent fluctuations [24, 44]. Properties of random matrix models thus provide a powerful heuristic tool, from which we may understand the properties of non-integrable systems analytically. In the remainder of this section, we will describe three key features of such systems, that may be understood from the ETH and RMT.

2.1. Thermalization

2.1.1. Equilibration to a thermal state. The first key feature of chaotic systems is the tendency in time to an equilibrium state described by a thermal ensemble. This has motivated the study of chaotic quantum systems as a fundamental description of the emergence of statistical physics from many-body dynamics [3, 45, 46]. The ETH describes sufficient conditions for thermalization of the long-time average value of an observable, which can be shown for an arbitrary initial state

$$|\phi_{\alpha_0}\rangle = \sum_\mu c_\mu(\alpha_0)|\psi_\mu\rangle, \tag{2}$$

where we use the index α_0 to identify the initial state for later convenience:

$$\begin{aligned}\overline{\langle O(t)\rangle} :&= \lim_{T\to\infty}\frac{1}{T}\int_0^T dt\langle O(t)\rangle \\ &= \lim_{T\to\infty}\frac{1}{T}\int_0^T dt\sum_{\mu,\nu} c_\mu(\alpha_0)c_\nu^*(\alpha_0)O_{\mu,\nu}e^{-i(E_\mu-E_\nu)t} \\ &= \sum_\mu |c_\mu(\alpha_0)|^2 O_{\mu,\nu} \approx \mathcal{O}(E_0),\end{aligned} \tag{3}$$

where E_0 is the initial state energy, and in the third line we have assumed there are no degenerate eigenenergies, and in the last line assumed the ETH, and that the initial state is not a macroscopic superposition, and thus the energy variance is small compared to macroscopic energies.

2.1.2. Long-time fluctuations. A second condition for thermalization to occur is the exponential vanishing of long-time fluctuations with system size. That is, after equilibration to a thermal state, fluctuations around this state in time should be small. We define the long-time fluctuations of an observable O as

$$\delta_O^2(\infty) := \lim_{T\to\infty}\left[\frac{1}{T}\int_0^T dt\langle O(t)\rangle^2 - \left(\frac{1}{T}\int_0^T dt\langle O(t)\rangle\right)^2\right]. \tag{4}$$

Assuming non-degenerate energies and energy gaps, we use the diagonal ensemble (DE) result [4, 28, 47],

$$\delta_O^2(\infty) = \sum_{\substack{\mu\nu \\ \mu\neq\nu}} |c_\mu(\alpha_0)|^2|c_\nu(\alpha_0)|^2|O_{\mu\nu}|^2. \tag{5}$$

Indeed, the size of fluctuations at long-times has been well studied in the ETH regime [4, 22, 24, 26, 48, 49], and in early works Reimann [27] and Short [50] provided bounds for the fluctuations in terms of some effective dimension of the state of the system. Here we use a similar effective system size, the inverse participation ratio (IPR) , defined by

$$\mathrm{IPR}(|\psi(0)\rangle) = \sum_{\mu} |\langle\psi_\mu|\psi(0)\rangle|^4, \tag{6}$$

which can be seen to have reasonable properties, as for a totally localized state, with $c_\mu(\alpha) = \delta_{\mu\alpha}$, we have, $\mathrm{IPR}(|\phi_\alpha\rangle) = 1$, and for a maximally delocalized state, with $c_\mu(\alpha) = \frac{1}{\sqrt{\dim(H)}}$, we have $\mathrm{IPR}(|\phi_\alpha\rangle) = \frac{1}{\dim(H)}$, where $\dim(H)$ is the dimension of the Hilbert space of the Hamiltonian. The (inverse of) the IPR is also often referred to as the 'number of principal components' [32, 49, 51] for this reason.

Recently [22], the current authors have obtained a relationship between the DE fluctuations and IPR from a RMT approach, finding that for observables which are diagonal in the basis of eigenstates of the non-interacting part of a chaotic Hamiltonian (which are our focus in the current work),

$$\delta_O^2(\infty) \propto \mathrm{IPR}(|\psi(0)\rangle). \tag{7}$$

The underlying assumption of this result is a coarse-graining of many-body eigenstates allowing for RMT methods to be applied. Crucially, it is assumed after this coarse-graining the eigenstates form a smooth function of energy. From this the ETH can be derived [22].

Indeed, both Reimann and Short's bounds can be understood in terms of the IPR, and equation (7) can be seen to follow the same scaling implied by a saturation of their bounds. This scaling of the fluctuations with system size has also been argued as a direct consequence of the ETH in (the supplemental material of) [15]. Further, this relation links the vanishing of long-time fluctuations with notions of ergodicity in terms of the explored Hilbert space dimension [52], which may be measured by the IPR.

2.2. Correlations

Here we discuss additional features of correlation functions that follow from the ETH, focussing on two-time correlation functions, and the OTOC. To make the link to the current work, where we focus on initial pure states, we note results of 'typicality' [53–55] imply that 'the overwhelming majority' of such initial pure states are representative of a relevant thermal ensemble [55]. We will see this numerically below, where we contrast our results for the correlated quench scenario to other physically relevant initial conditions.

2.2.1. Two-time correlations. The behaviour of two-time correlation functions, $\langle O(t)O\rangle$, is of fundamental and practical importance to the study of many-body systems, providing a foundation for linear response theory [56], open quantum systems [57], and many other approaches. The factorization of two-time correlation functions,

$$\langle W(t\to\infty)V\rangle_{\mathrm{ens}} = \langle W\rangle_{\mathrm{ens}}\langle V\rangle_{\mathrm{ens}} \tag{8}$$

where $\langle\cdots\rangle_{\mathrm{ens}}$ denotes an average with respect to a relevant ensemble, is a fundamental result describing dissipative processes in quantum and classical systems. Theorems describing the factorization of two-time correlations has been derived from the ETH for both microcanonical [58] and thermal [33] states. The former case is shown to follow directly from the diagonal ETH, and in the latter case, a weak version of the ETH is assumed, as well as non-degeneracy

of energy levels, and correlation function factorisation is observed up to an error term that is vanishingly small in most relevant cases.

In the following we refer to initial states of a system that result in a factorization of two-time correlators at long times as ergodic. We note for a fixed initial state and Hamiltonian, there may be factorising and non-factorising (ergodic and non-ergodic) observables; hence, ergodicity is a property of the combined state, Hamiltonian, and observable.

2.2.2. Scrambling of quantum information. In classical mechanics, chaos is identified by the exponential divergence of trajectories at a rate given by the Lyapunov exponent. That is, take an initial state, and a slightly perturbed copy—under chaotic time evolution these states exponentially diverge.

Chaos may similarly be measured in a quantum system by the spreading of local information about a state over the entire system in time. This can be measured, for example, by the evolution of a local observable $W(t) = e^{iHt}We^{-iHt}$, and the effect of a local perturbation V, by the so-called OTOC [51, 59–65], defined as,

$$F(t) = \langle W^\dagger(t)V^\dagger W(t)V\rangle. \tag{9}$$

Information scrambling refers to the spreading of local information over the degrees of freedom of a system, and is related to the chaoticity of quantum systems [59]. The OTOC can be seen to be related to the commutator

$$C(t) := \langle|[W(t),V]|^2\rangle = 2\left(1 - \mathrm{Re}[F(t)]\right), \tag{10}$$

for unitary W, V. For non-unitary W, V, there are additional time-ordered correlator terms in the $C(t)$. As scrambling of quantum information occurs as local information is delocalized over the many-body system, two initially commuting observables, $[W(0),V] = 0$, should have a non-zero commutator at some later time in a scrambling system. It can thus be seen that the OTOC, $F(t)$, is related to the growth of the support of localized operators in time, and information scrambling will cause $F(t)$ to decay.

As alluded above, the OTOC can be related to chaos in an analogous manner to the definition of a Lyapunov exponent in classical systems. In a chaotic quantum system at short times, the OTOC is expected to take the form [62],

$$F(t) \approx 1 - \epsilon e^{-\lambda_L t}, \tag{11}$$

where λ_L is conjectured to be a quantum analogue of the Lyapunov exponent. The link between quantum chaos as defined by the ETH, and the behaviour of the OTOC in equation (11) is not yet totally clear, however some important steps have been made in e.g. linking the ETH to known bounds on λ_L [66].

In the following we limit our attention to the long-time average, defined by $\overline{F} := \lim_{T\to\infty}\frac{1}{T}\int_0^T dtF(t)$, which is expected to be equal to zero for chaotic systems. This may be seen for example from relating chaotic dynamics to random unitaries [67], and more directly as a consequence of the ETH [64]. We will see that when both the ergodicity relation (8), and the scaling of fluctuations equation (7), deviate from the ETH predictions, we similarly see a deviation of the long-time average $\overline{F}$ from the expected value of zero for chaotic systems.

Generally, the expectation value $\langle\cdots\rangle$ is taken at some inverse temperature β, such that $\langle\cdots\rangle = tr(\rho\cdots)$, with $\rho_{\mu\nu} = \frac{1}{Z}e^{-\beta E_\mu}\delta_{\mu\nu}$, and Z is the partition function. Here, however, we

focus on initial pure states, and thus use $\langle\cdots\rangle = \langle\psi|\cdots|\psi\rangle$ for some state $|\psi\rangle$. $\overline{F}$ may be then written as,

$$\begin{aligned}\overline{F} &= \overline{\langle\phi_{\alpha_0}|W^\dagger(t)V^\dagger W(t)V|\phi_{\alpha_0}\rangle} \\ &= \sum_{\mu\nu} c_\mu(\alpha_0)c_\nu(\alpha_0)\overline{\langle\psi_\mu|W^\dagger(t)V^\dagger W(t)V|\psi_\nu\rangle},\end{aligned} \tag{12}$$

for an initial state given by equation (2). We assume time reversal symmetry, such that the $c_\mu(\alpha)$s may be taken as real, though one can easily see our approach extends to the non time-reversal symmetric case.

We note it has been previously observed that scrambling is somewhat state-dependent [40, 63, 68], even in non-integrable systems—and we may expect a similar behaviour for two-time correlation functions—where initial pure states may deviate from the ETH result. The following results can be understood in the context of the ETH understanding that it necessarily omits eigenstate correlations—this has been previously shown to have an impact in terms of spatial correlations [69]; the following results can be seen as a consequence of energetic correlations between the initial state, Hamiltonian, and observable.

3. Set up

In this section we describe, and give a simple example of, the correlated quench scenario in which we observe a discrepancy from the markers of chaoticity in quantum systems. We will show this as a simple example of where one expects the scaling of fluctuations to differ from equation (7), and outline more formally conditions where we expect this behaviour generally.

3.1. Simple example

We consider first a simple case of L two level systems (qubits) with a Hamiltonian in the form $H = H_\mathrm{S} + H_\mathrm{B} + H_\mathrm{SB}$, which conserves the total number of excited qubits, $\hat{N} = \sum_i^N \frac{1}{2}(\sigma_z^{(i)} + \mathbb{1})$, where $\sigma^{(i)}_{\{x,y,z\}}$ are the Pauli matrices acting on site i. We initialize the system in the state $|\psi(0)\rangle = |\uparrow\rangle_\mathrm{S}\prod_i^{\mathcal{N}_\mathrm{B}}|\downarrow\rangle_{\mathrm{B},i}$. We thus see the time evolution is restricted to the subspace of a single excitation only, as depicted in figure 1.

If we initialize our system in the state,

$$|\psi(0)\rangle = |\uparrow\rangle_\mathrm{S}|k_0\rangle_\mathrm{B}, \tag{13}$$

where $|k_\alpha\rangle_\mathrm{B}$ denote eigenstates of $\hat{N}_\mathrm{B}$, and $|k_0\rangle_\mathrm{B}$ specifies a particular non-degenerate eigenstate of the conserved quantity $\hat{N}_\mathrm{B}$, such as that with zero excitations, $N_\mathrm{B} = 0$. We thus have $\langle\hat{N}\rangle = 1$. Now, we have that eigenstates of H_0 are given by $|\phi_\alpha\rangle = |s_\alpha\rangle_\mathrm{S}|k_\alpha\rangle_\mathrm{B}$, where $s_\alpha = \{\uparrow,\downarrow\}$ is simultaneously an eigenstate of the conserved quantity $\hat{N}$. For example, if in a system of L qubits $\hat{N} = \sum_i^N \frac{1}{2}(\sigma_z^{(i)} + \mathbb{1})$ is conserved, then we may have $|\phi_\alpha\rangle = |\uparrow,\downarrow,\cdots\rangle$, and the conserved quantity is the total number of qubits in the up and down states.

The survival probability of the initial state can be written as the expectation value of the operator P_0, where,

$$P_0 = |\psi(0)\rangle\langle\psi(0)| = \sum_{\mu,\nu} c_\mu(\alpha_0)c_\nu(\alpha_0)|\psi_\mu\rangle\langle\psi_\nu|, \tag{14}$$

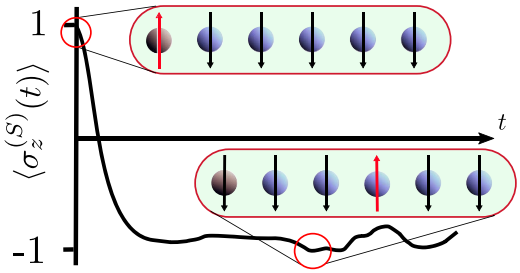

Figure 1. Idealised scenario of a correlated quench. It shows an initial state with a single spin excitation in the system and all spins in the bath in the zero excitation state. If we assume the number of excitations $\hat{N}$ is conserved, then at later times the system spin is more likely to be in the ground state and a single excitation propagates in the bath. Note that the initial bath state is not necessarily the ground state of H_{B}.

where $|\psi_\mu\rangle$ is an eigenstate of H, the initial state is given by equation (2). We thus have $(P_0)_{\mu\nu} = c_\mu(\alpha)c_\nu(\alpha)$, and thus the fluctuations, equation (5), can be written as

$$\begin{aligned}\delta^2_{P_0}(\infty) &= \sum_{\substack{\mu\nu \\ \mu\neq\nu}} |c_\mu(\alpha_0)|^2|c_\nu(\alpha_0)|^2(c_\mu(\alpha_0)c_\nu(\alpha_0))^2 \\ &= \sum_{\mu\nu} |c_\mu(\alpha_0)|^4|c_\nu(\alpha_0)|^4 - \sum_\mu |c_\mu(\alpha_0)|^8 \\ &\approx \mathrm{IPR}(|\psi(0)\rangle)^2,\end{aligned} \tag{15}$$

where in the last line we have used that many-body eigenstates of the systems of interest have a small IPR, and thus $\max c_\mu(\alpha) \ll 1$.

One can thus see for the survival probability, we do not observe the scaling of fluctuations of equation (7), predicted by RMT and the ETH. Indeed, it has recently been shown that the survival probability is not 'self-averaging' [70], which implies it may not be expected to follow RMT behaviour at any time scale. Of particular note is that for the scenario outlined above, the dynamics of $\hat{N}$ and P_0 are strictly proportional to one another (as will be shown in more detail below), and thus the scaling of fluctuations of $\hat{N}$ must similarly deviate from the ETH result.

In this simple example lies the key intuition of the main result of this work, which we formulate in a more general scenario below. That is, for certain initial states and observables related to a conservation law, the long-time behaviour of the observable deviates from the expected behaviour due to the ETH. Here we have seen this for the example of observable fluctuations, however the more general treatment below will further analyse the behaviour of two- and four-point correlation functions.

We once again stress that these results apply to systems which may in general obey the ETH. Indeed, in the example above H may obey the ETH in each symmetry sector. Our result suggests the introduction of a symmetry allows for correlations between the observable and initial state to dominate dynamics. It is these correlations that deviate the long-time behaviour from the expected by relations implied by the ETH.

3.2. Formal conditions

In the following, we focus on models described by a Hamiltonian of the form $H = H_S + H_B + H_{SB}$, where H_S is a 2×2 Hamiltonian of a single qubit, with eigenstates $\{|\uparrow\rangle_S, |\downarrow\rangle_S\}$. We discuss in appendix C how these ideas scale to larger system Hamiltonians, noting that this is non-trivial, but can be expected in some generic settings. We use subscripts S and B to refer to the system and bath respectively. The subscript SB denotes coupling terms between these subsystems.

A crucial condition of the discussion in the previous section is the presence of some conservation law $[H, \hat{A}] = 0$. We further require the operator $\hat{A} = \hat{A}_S + \hat{A}_B$ is the sum of at least two local operators defined separately on the system and bath. These local operators are each conserved in both the system and bath under the non-interacting Hamiltonian $H_S + H_B$, such that $[H_S, \hat{A}_S] = 0$, and $[H_B, \hat{A}_B] = 0$, yet are not conserved by the total system Hamiltonian $[H, \hat{A}_S] \neq 0$, $[H, \hat{A}_B] \neq 0$. We study the behaviour of a local observable O_S that is diagonal in the basis of the local excitation number, and thus $[O_S, \hat{N}_S] = [O_S, H_S] = 0$.

The second key condition applies to the initial state. We require the initial bath state is a non-degenerate state of the quantity $\hat{A}_B$, implying there is a single state with the eigenvalue ${}_B\langle\psi(0)|\hat{A}_B|\psi(0)\rangle_B = A_B$. The system is initialized in the excited state of $\hat{A}_S$ (and thus of H_S). This ensures that, after measurement of O_S, if the system is found to be in the initial state, there is only a single excitation configuration possible for the bath state. This is guaranteed by choosing an initial state where there is a single excitation, localized to the system qubit.

To summarize, then, we focus on the behaviour of non-integrable systems under the following conditions: (a) a conserved charge or excitation number, (b) the local system observable is diagonal in the basis of the local excitation number, (c) the initial state has a single excitation localized to the system. We will see below that these conditions are enough to identify a local observable with the survival probability (up to some constant factor), and thus ensure the behaviour of the observable violates the ETH results of section 2, yet still thermalizes for systems with a large effective dimension (small IPR).

In the following, we will refer to the thermalization under the above conditions as a 'correlated quench'. We note these conditions are indeed particularly restrictive. We stress, however, such specificity is to be expected—conditions in non-integrable systems that violate the ETH should be exceptionally rare. Further, as more symmetries are included, these conditions are not so stringent, as many more initial states fulfil them. This approach thus also contributes to a generic understanding of aspects of the behaviour of integrable and near integrable models, where conserved quantities dominate the dynamics. We further note that these conditions are applicable to many cases of interest, such as the spin-boson model, which we discuss in appendix A, and are observed to be robust to perturbations away from strict fulfilment of the conditions above, as shown in appendix D.

4. Fluctuations and observable elements

Here we once more focus on the case where the system is a single qubit with Hamiltonian H_S with eigenstates $\{|\uparrow\rangle_S, |\downarrow\rangle_S\}$, and treat a bath Hamiltonian H_B with symmetry $[H_B, \hat{N}_B] = 0$, with the total system initialised in the state equation (13).

We begin by expanding the many-body eigenstate of $H = H_S + H_B + H_{SB}$, $|\psi_\mu\rangle$, noting that the terms may be separated into two types, those with the system in each of its two eigenstates $|\uparrow\rangle_S$ and $|\downarrow\rangle_S$. Each part is then a sum over the bath states k (writing $c_\mu(\alpha) := c_\mu(k_\alpha, s_\alpha)$),

$$|\psi_\mu\rangle = \sum_k c_\mu(k,\uparrow)|\uparrow\rangle_S|k\rangle_B + \sum_k c_\mu(k,\downarrow)|\downarrow\rangle_S|k\rangle_B, \tag{16}$$

where we have dropped the subscript α. Now, for a local system observable $O = O_S \otimes \mathbb{1}_B$ we have, for example, that ${}_B\langle k|_S\langle\uparrow|O|\uparrow\rangle_S|j\rangle_B = O_{\uparrow\uparrow}\delta_{kj}$, where $O_{\uparrow\uparrow} := {}_S\langle\uparrow|O_S|\uparrow\rangle_S$, and $O_{\downarrow\downarrow} := {}_S\langle\downarrow|O_S|\downarrow\rangle_S$. Thus, the matrix elements $O_{\mu\nu}$ may be expressed as

$$\begin{aligned} O_{\mu\nu} = &\sum_k c_\mu(k,\uparrow)c_\nu(k,\uparrow)O_{\uparrow\uparrow} + \sum_k c_\mu(k,\downarrow)c_\nu(k,\downarrow)O_{\downarrow\downarrow} \\ &+ \sum_k c_\mu(k,\uparrow)c_\nu(k,\downarrow)(O_{\uparrow\downarrow} + O_{\downarrow\uparrow}). \end{aligned} \tag{17}$$

We can further use that

$$\begin{aligned} \sum_k c_\mu(k,\downarrow)c_\nu(k,\downarrow) &:= \sum_k \langle\psi_\mu|\Big(|\downarrow\rangle_S|k\rangle_{BB}\langle k|_S\langle\downarrow|\Big)|\psi_\nu\rangle \\ &= \langle\psi_\mu|\Big(\mathbb{1} - \sum_k |\uparrow\rangle_S|k\rangle_{BB}\langle k|_S\langle\uparrow|\Big)|\psi_\nu\rangle \\ &= \delta_{\mu\nu} - \sum_k c_\mu(k,\uparrow)c_\nu(k,\uparrow), \end{aligned} \tag{18}$$

where we have used the completeness relation $\sum_\alpha |\phi_\alpha\rangle\langle\phi_\alpha| = \mathbb{1}$, to obtain, for the case of an observable that commutes with the local excitation number (such that $O_{\uparrow\downarrow} = 0$),

$$O_{\mu\nu} = \Delta O \sum_k c_\mu(k,\uparrow)c_\nu(k,\uparrow) + O_{\downarrow\downarrow}\delta_{\mu\nu}, \tag{19}$$

where we have defined $\Delta O := O_{\uparrow\uparrow} - O_{\downarrow\downarrow}$.

To gain an understanding of the effect of the conservation law, we can estimate the value of time-fluctuations assuming that the system is in the initial state (13),

$$\begin{aligned} \delta^2_O(\infty) = &\sum_{\substack{\mu,\nu \\ \mu\neq\nu}} |c_\mu(\uparrow,k_0)|^2|c_\nu(\uparrow,k_0)|^2 \\ &\times \Delta O^2|\sum_k c_\mu(k,\uparrow)c_\nu(k,\uparrow)|^2. \end{aligned} \tag{20}$$

One could naively assume that wave function components $c_\mu(k,\uparrow)$ and $c_\mu(k_0,\uparrow)$ are just independent random variables and carry out the summation. However, if we assume that the coupling term conserves the total number of excitations,N_{ex}, then the sum over μ, ν, must run over values with $N_{ex} = 1$. Thus, the components $c_\mu(k,\uparrow)$ can only take non-zero values if $k,\uparrow$ corresponds to a total excitation value $N_{ex} = 1$. Thus, the sum is restricted to $k = k_0$.

Concretely, then, we can see that the summation

$$\eta = \sum_k c_\mu(k,\uparrow)c_\nu(k,\uparrow), \tag{21}$$

may be restricted simply to the term,

$$\eta = c_\mu(k_0,\uparrow)c_\nu(k_0,\uparrow) := c_\mu(\alpha_0)c_\nu(\alpha_0), \tag{22}$$

where we have defined $\alpha_0 = (k_0,\uparrow)$ as the indices of the initial state.

This then leads us to the form for observable matrix elements,

$$O_{\mu\nu} = \Delta O c_\mu(\alpha_0)c_\nu(\alpha_0) + O_{\downarrow\downarrow}\delta_{\mu\nu}. \tag{23}$$

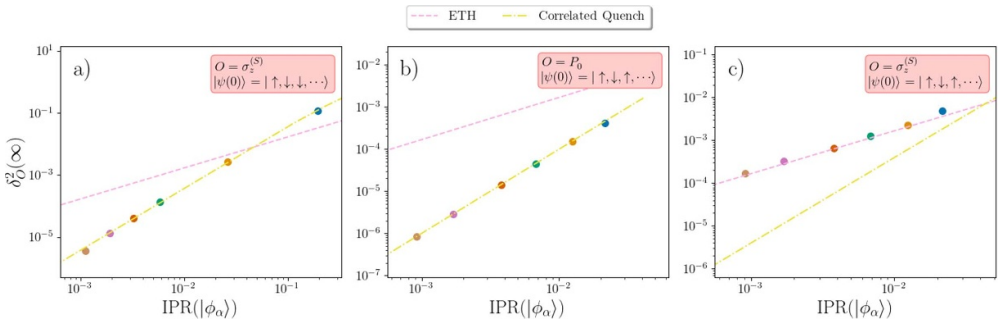

Figure 2. DE Fluctuations versus IPR for Hamiltonian (26) and (27). Observables are $\sigma_z^{(S)}$ for (a), (c) and P_0 for (b). Initial bath states are all qubits down for (a), and the Neel state for (b), (c). Values of increase with decreasing IPR and fluctuations, and are $N = [10, 100, 500, 1000, 2000, 5000]$ for (a), and $N = [10, 11, 12, 13, 14, 15]$ for (b), (c). These are chosen such that the IPR values are roughly similar, noting that the correlated quench dynamics takes place in a significantly reduced subspace. 'ETH' and 'Correlated Quench' label the expected scalings of equations (7) and (24), respectively. Parameters: $B_z = 0.05$, $J = 1$, $J' = 0.8$.

Here we note that this relation is not expected for all matrix elements $O_{\mu\nu}$, which in general may in-fact still obey the ETH, and thus take the form of equation (1). Rather, here we have that the few matrix elements of particular observables accessible from the described initial state are restricted to the form above, and thus these matrix elements obey a different relation. One can see that this recovers the form of Srednicki's ansatz [26] if $c_\mu(\alpha_0)c_\nu(\alpha_0)$ is taken to be a suitably small stochastic variable, however, equation (23) allows for correlations between the wave function coefficients $c_\mu(k, \uparrow)$, to be included.

In understanding equation (23) it is thus important to stress that the observable matrix elements are indeed still in reality described by equation (19), however, due to the conserved quantity $\hat{N}$ and correlated initial state the dynamics are restricted to a subset of the Hilbert space. It is precisely this restriction that allows us to make the substitution (23).

Applying equation (23) to the long-time fluctuations, we thus obtain,

$$\begin{aligned}\delta_O^2(\infty) &= \Delta O^2 \sum_{\substack{\mu\nu \\ \mu\neq\nu}} |c_\mu(\alpha_0)|^2 |c_\nu(\alpha_0)|^2 (c_\mu(\alpha_0)c_\nu(\alpha_0))^2 \\ &= \Delta O^2 \sum_{\mu\nu} |c_\mu(\alpha_0)|^4 |c_\nu(\alpha_0)|^4 - \Delta O^2 \sum_\mu |c_\mu(\alpha_0)|^8 \\ &\approx \Delta O^2 \mathrm{IPR}(|\psi(0)\rangle)^2,\end{aligned} \tag{24}$$

where we have once more assumed a small IPR, which implies $\sum_\mu |c_\mu(\alpha_0)|^8 \ll (\sum_\mu |c_\mu(\alpha_0)|^4)^2$. We thus recover the same scaling of fluctuations as seen in general for the survival probability, which differs from the ETH.

We numerically confirm this approach in a quantum spin-chain model, described below, in figure 2, where it is contrasted to the behaviour of a different initial state that is a highly degenerate eigenstate of H_B. We observe that the system observable scales as expected by (7) in this case, whereas the survival probability fluctuations deviate from the ETH for all initial states. In appendix A we study the spin-boson model, and see the same scaling can be derived for this model in the rotating wave approximation (RWA).

Further, in appendix D we show a case where this scaling is obtained without the conservation of excitation number when the initial state is the ground state of a non-interacting Hamiltonian prior to a quantum quench. Intuitively, this can be seen as a by-product instead of conservation of energy; in cases where additional excitations require an additional energy cost, such transitions only contribute weakly, and equation (23) holds approximately.

5. Two-point correlators

In this section we will see that the long-time behaviour of the two-point correlators of the correlated quench procedure indeed deviates from the expected factorisation, equation (8). This can be seen using equation (23):

$$\begin{aligned}\overline{\langle O(t)O\rangle} &= \sum_{\mu\nu} c_\mu(\alpha_0)c_\nu(\alpha_0)O_{\mu\mu}O_{\mu\nu}\\ &= \sum_{\mu\nu} c_\mu(\alpha_0)c_\nu(\alpha_0)(\Delta O c_\mu(\alpha_0)c_\nu(\alpha_0)+O_{\downarrow\downarrow})\\ &\quad\times(\Delta O c_\mu(\alpha_0)c_\nu(\alpha_0)+O_{\downarrow\downarrow}\delta_{\mu\nu})\\ &= \Delta O^2\mathrm{IPR}(|\phi_{\alpha_0}\rangle)+O_{\downarrow\downarrow}^2\\ &\quad+\Delta O O_{\downarrow\downarrow}(1+\mathrm{IPR}(|\phi_{\alpha_0}\rangle)\\ &\approx O_{\uparrow\uparrow}O_{\downarrow\downarrow}\\ &\neq O_{\downarrow\downarrow}^2,\end{aligned} \tag{25}$$

where in the penultimate line we have assumed, as above, that the initial state is spread over a large number of many-body eigenstates, and thus the IPR is small. The last inequality highlights the deviation of the long-time average from that implied by the ETH $O_{\mathrm{MC}}^2 \approx O_{\downarrow\downarrow}^2$. This is shown in figure 3(a) for the spin-chain model described in the next section.

6. Numerical model

For our numerical calculations we use a non-integrable spin-chain model, where the bath is given by the XXX chain with nearest and next-nearest neighbour couplings (NN-XXX). Our system qubit is 'biased' with a small B_z component. The Hamiltonian is written in the form $H = H_0 + H_I$, with

$$H_0 = B_z^{(0)}\sigma_z^{(0)} + \sum_{\langle\alpha,\beta\rangle>0} J\boldsymbol{\sigma}_\alpha\cdot\boldsymbol{\sigma}_\beta, \tag{26}$$

where we set the system index equal to zero, such that $H_{\mathrm{S}} = B_z^{(0)}\sigma_z^{(0)}$, and,

$$H_I = J\boldsymbol{\sigma}_0\cdot\boldsymbol{\sigma}_1 + \sum_{\langle\langle\alpha,\beta\rangle\rangle} J'\boldsymbol{\sigma}_\alpha\cdot\boldsymbol{\sigma}_\beta, \tag{27}$$

where $\boldsymbol{\sigma_\alpha} = (\sigma_x^{(\alpha)},\sigma_y^{(\alpha)},\sigma_z^{(\alpha)})$, and $\langle\cdots\rangle$ and $\langle\langle\cdots\rangle\rangle$ indicate summations over nearest neighbours and next-nearest neighbours of the respectively. H_0 thus describes a system qubit placed at one end of the chain, uncoupled from an XXX chain with nearest-neighbour interactions only. The action of H_I is to couple the system qubit to both it is neighbour and next-nearest neighbour, as well as include next-nearest neighbour interactions throughout the chain. The system is thus homogeneous, except for a small 'bias' field on the system qubit only, acting to ensure the initial state is an excited eigenstate of the conserved quantity $\hat{N}_{\mathrm{S}} = \sigma_z^{(\mathrm{S})}$. The total

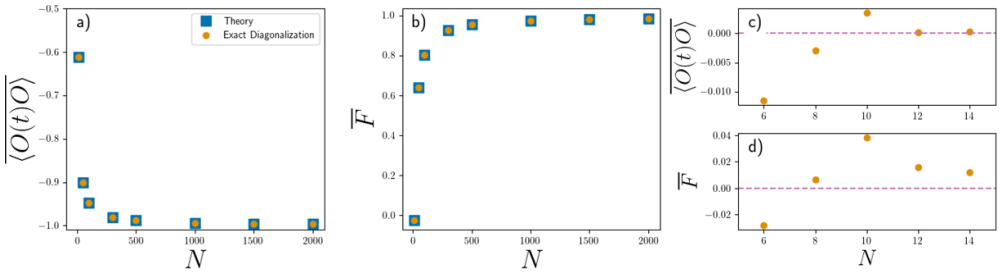

Figure 3. Exact diagonalization calculations of long time average of correlation functions for varying initial states and number of qubits L for the NN-XXX model (equations (26) and (27)). (a) $\overline{\langle O(t)O\rangle}$ given in equation (25) for initial All Down state, satisfying the correlated quench. Theory (blue squares) calculated from correlated quench assumption equation (24), and Exact Diagonalization (yellow circles) from equation (5). (b) Long-time OTOC for initial All Down state. Theory (blue squares) and Exact Diagonalization (yellow circles) calculated from equations (30) and (B1), respectively. (c) and (d) show long time values of $\overline{\langle O(t)O\rangle}$ and OTOC, respectively, for an initial Neel state. Magenta dashed line shows expected result from ETH as discussed in section 2. Even values of N Neel state shown such that the initial state has the same number of up and down spins. $B_z = 0.05$, $J = 1$, $J' = 0.8$.

conserved quantity is the total magnetization $\sum_i \sigma_z^{(i)}$, such that the number of excitations is given by $\hat{N} = \sum_i \frac{1}{2}(\sigma_z^{(i)} + \mathbb{1})$.

This model is chosen for it is resemblance (up to the system B_z field) to the model of [63], where the lack of scrambling of quantum information was observed for states with such a conservation law. We argue that equation (23) can be seen as the mechanism behind this observation, seeing that scrambling is not violated simply due to a confined subspace by the conservation law, but rather that the mixing of eigenstates in time evolutions is restricted, and thus off-diagonal observable matrix elements may not be treated as random.

Our numerical results are shown in figure 2, where we have investigated the NN-XXX model for the observable $\sigma_z^{(\mathrm{S})}$, with initial bath states as the correlated initial state $|\downarrow,\downarrow,\cdots\rangle_{\mathrm{B}}$ (All down), figure 2(a), and both the survival probability, P_0 and $\sigma_z^{(\mathrm{S})}$ for a highly degenerate product state, $|\uparrow,\downarrow,\cdots\rangle_B$ (Neel), figures 2(b) and (c), respectively. Here we observe that for the correlated initial state the local observable $\sigma_z^{(\mathrm{S})}$ follows the scaling of equation (24) as expected from the arguments above. We further see the survival probability follows this scaling exactly for all initial states.

We note that the Hilbert space dimension available to the initial states in each scenario scale vastly differently with system size. As the Hamiltonian conserves excitation number, we restrict to the relevant subspace for numerical exact diagonalization. The All down state for the correlated quench scales only linearly with system size, and thus we can access far larger systems. We choose values for each with similar IPRs, such that the initial state is similarly distributed over many-body eigenstates. We additionally note this initial state is not particularly close to the ground state of the Hamiltonian, due to the energy bias on the system qubit. For example, for $L = 1000$, and rescaling the energies to the range [0, 1], the initial state has an energy expectation value of ~ 0.73 for $B_z = 0.05, J = 1, J' = 0.8$, which are the parameters used in numerical results shown.

We have used the Neel state as a reference state as it has the same system state, yet the bath state has many possible confirmations that conserve $\hat{N}_{\mathrm{B}}$, thus, one cannot make the assumptions following equation (13), and such the observable fluctuations should obey the ETH.

7. Time evolution

The time dependence of an observable O of a closed quantum system initialized by the state given in equation (13) may be written as

$$\begin{aligned}\langle O(t)\rangle &= \sum_{\mu\nu} c_\mu(\alpha_0)c_\nu(\alpha_0)e^{-i(E_\mu-E_\nu)t}O_{\mu\nu} \\ &= \Delta O\sum_{\mu\nu}|c_\mu(\alpha_0)|^2|c_\nu(\alpha_0)|^2e^{-i(E_\mu-E_\nu)t} \\ &\quad + O_{\downarrow\downarrow}\sum_\mu c_\mu^2(k_0,\uparrow),\end{aligned} \tag{28}$$

where in the second line we have applied equation (23). We thus obtain

$$\langle O(t)\rangle = \Delta O P_0(t) + O_{\downarrow\downarrow}, \tag{29}$$

where $P_0 = |\langle\psi(0)|\psi(t)\rangle|^2 = \sum_{\mu\nu}|c_\mu(\alpha_0)|^2|c_\nu(\alpha_0)|^2e^{-i(E_\mu-E_\nu)t}$ is the survival probability. This may be understood as a special case of the results of references [23, 24, 71].

This is corroborated in figure 4. Note that the case of the correlated quench follows the survival probability dynamics strikingly closely, even faithfully reproducing its fluctuations.

8. Long-time OTOC

Exploiting equation (23), the long time OTOC, may be obtained by calculation of equation (12). This is a somewhat tedious calculation, shown in full in appendix B. We obtain,

$$\begin{aligned}\overline{F(t)} &= W_\downarrow^2V_\downarrow^2 + W_\downarrow^2\Delta VV_\downarrow + W_\downarrow^2\Delta V^2 + W_\downarrow^2\Delta VV_\downarrow\mathcal{I}_4[4\Delta WW_\downarrow\Delta VV_\downarrow \\ &\quad + 2\Delta WW_\downarrow V_\downarrow^2 + 2\Delta W^2W_\downarrow\Delta V^2 + \Delta W^2V_\downarrow^2 + \Delta W^2\Delta VV_\downarrow] \\ &\quad + \mathcal{I}_4^2[2\Delta W^2\Delta VV_\downarrow + 2\Delta W^2\Delta V^2] - \mathcal{I}_8[\Delta W^2\Delta V^2 + \Delta W^2\Delta VV_\downarrow],\end{aligned} \tag{30}$$

where $\mathcal{I}_n := \sum_\mu c_\mu^n(\alpha_0)$, and thus $\mathcal{I}_4 = \mathrm{IPR}(|\phi_0\rangle)$. Here we have used notation as described above equation (17) for observables W and V replacing O. In the limit of large system size, where the IPR is small, this thus simplifies to

$$\overline{F(t)} \approx W_\downarrow^2V_\downarrow^2 + W_\downarrow^2\Delta VV_\downarrow + W_\downarrow^2\Delta V^2 + W_\downarrow^2\Delta VV_\downarrow, \tag{31}$$

which is equal to unity for $W = V = \sigma_z^{(S)}$, implying that the information on this local observable is *not-scrambled*, even for large non-integrable Hamiltonians.

In figure 3(b) we observe the behaviour of the long time value $\overline{F}$ for the initial correlated state. We see that, indeed, $\overline{F}$ does not indicate the scrambling of information, and is exactly in agreement with equation (30).

This indicates that the dynamics of the system after a correlated quench procedure is non-chaotic. The fact that this system behaves non-chaotically motivates the relation to an integrable system i.e. a system with an extensive number of conserved quantities. Our approach thus provides some intuition on the transition to integrability, upon which an extensive number of initial states will behave as above. To further understand this intuition, we note that in [72] it was shown that even integrable systems may display ETH-like behaviour (where long-time dynamics is effectively generated an unbiased sampling of Hamiltonian eigenstates) for chaotic initial states (eigenstates of a non-integrable model). Non-ergodic states of integrable

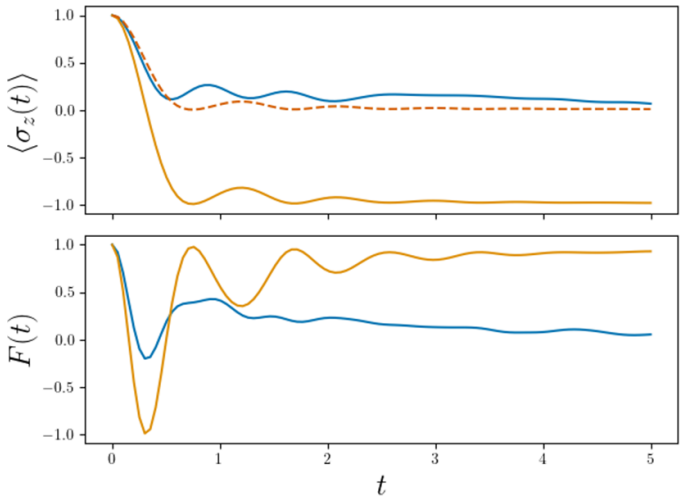

Figure 4. Dynamics of the NN-XXX model (equations (26) and (27)) for (a) observable $\sigma_z^{(S)}$ (orange solid line) and P_0 (orange dashed line) for an initial All down state $|\psi(0)\rangle = |\uparrow,\downarrow,\downarrow,\downarrow\cdots\rangle$ and observable $\sigma_z^{(S)}$ for initial Neel state $|\psi(0)\rangle = |\uparrow,\downarrow,\uparrow,\downarrow,\cdots\rangle$. The dynamics after a correlated quench can be seen to closely follow the survival probability, and decays to an equilibrium value $\sim O_{\downarrow\downarrow} = -1$, as expected by equation (29). (b) Shows dynamics of $F(t)$ for $W = V = \sigma_z^{(S)}$ for All down (orange line) and Neel (blue line) states. $B_z = 0.05, J = 1, J' = 0.8, N = 15$.

systems are thus not ubiquitous, but rather they are defined by their relation to the extensive number of Hamiltonian symmetries. The correlated quench describes a mechanism by which some of these non-ergodic states in integrable systems may emerge.

9. Discussion

In this article we have observed and obtained the mechanism behind a scenario in which quantum thermalization occurs in generic chaotic systems, yet other predictions of the ETH are violated due to correlations between the initial state, observable, and a symmetry of the system. The scenario in question we have called a 'correlated quench', where the bath is initially in a non-degenerate state with respect to some conservation law. We observe for given local system observables, thermalization occurs without the full ETH, as the off-diagonal observable elements can be seen to be non-random, as correlations dominate both long and short time behaviour of the observable. Indeed, from the derived expression for off-diagonal observable elements, we have analytically obtained the long-time fluctuations and time evolution of observables, as well as the long time value of the OTOC.

The correlated quench requires particular conditions that are nonetheless quite common in physical scenarios; relying on correlations between the initial state, observable, and some Hamiltonian symmetry. Product state initial states with a ground-state bath are a particular example, though we note the initial state energy need not be close to the ground state itself (indeed the ETH is not expected to apply close to the edges), as the observed deviations of the ETH are exact due to symmetry conditions. We have further seen the phenomena observed

in a correlated quench are robust to perturbations, such as additional excitations of the initial state, or excitation non-conserving terms in the Hamiltonian. In this case, the ETH results are recovered either as the system size or perturbation strength are increased.

The time evolution of observables after a correlated quench follows that of the survival probability closely, which provides a potential method of measuring the survival probability itself. This is useful, for example, as it is Fourier transform is the so-called local density of states, or strength function. Thus our results imply this may be measured using such a correlated quench protocol.

The arguments outlined above rest on the behaviour of the parameter η, equation (21). This parameter dictates the available states that may mix with the initial state in time evolution. It is thus an important quantity in dictating the ergodicity of a quantum system, or it is ability to scramble quantum information.

Data availability statement

The data that support the findings of this study are available upon reasonable request from the authors.

Acknowledgments

C N would like to thank C B Dağ for enlightening discussions. We acknowledge funding by EPSRC Grant No. EP/M508172/1, Project PGC2018-094792-B-I00 (MCIU/AEI/FEDER, UE), the Gordon and Betty Moore Foundation Projects GBMF8820 and TIPICQA (COST Action CA17113).

Appendix A. Relation to the rotating wave approximation—the spin-boson model

In this section we give an example of the scaling of time-averaged fluctuations for an integrable spin-boson model. This model serves to provide intuition on the origin of the deviations from the ETH observed in the main text, which will carry over in a straight-forward manner to more general systems. We will see here that the excitation conservation law is equivalent to the RWA in the familiar model of a single spin coupled to a Bosonic bath.

The model we discuss is the spin-boson model, which we may write as

$$H = H_{\mathrm{S}} + H_{\mathrm{B}} + H_{\mathrm{SB}}, \tag{A1}$$

with

$$H_0 = H_{\mathrm{S}} + H_{\mathrm{B}} = \frac{\omega_z}{2}\sigma_z + \sum_n \omega_n a_n^\dagger a_n, \tag{A2}$$

and

$$H_{\mathrm{SB}} = \sum_n g_n (a_n + a_n^\dagger)(\sigma_+ + \sigma_-), \tag{A3}$$

where σ_i $i = x,y,z$ are the Pauli operators, $\sigma_\pm = \frac{1}{2}(\sigma_x \pm i\sigma_y)$, and $a_n^\dagger(a_n)$ are creation (annihilation) operators of a boson in state n. Making the RWA, and thus ignoring counter rotating terms $a_n\sigma_-$ and $a^\dagger\sigma_+$, we obtain

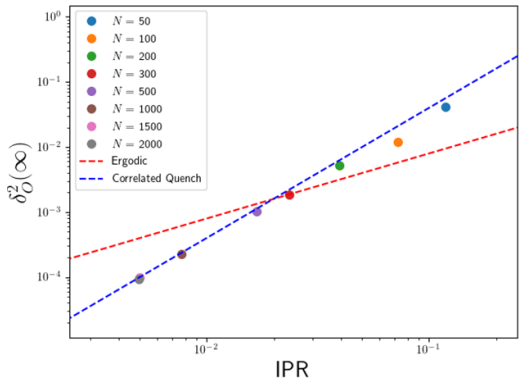

Figure 5. DE Fluctuations versus IPR for spin-boson model equation (A1) with $\omega_z = 0.6, \Gamma = \frac{2\pi g^2}{\omega_0} = 0.1, \omega_n = n\omega_0 = \frac{n}{N}$. g_n is a random number with mean zero and variance g.

$$H_{\mathrm{SB}} = \sum_n g_n (a_n \sigma_+ + a_n^\dagger \sigma_-). \tag{A4}$$

We can thus see that the total Hamiltonian conserves the total number of excitations $\hat{N} = \frac{1}{2}(\sigma_z + \mathbb{1}) + \sum_n a_n^\dagger a_n$. We thus initiate a correlated quench, such that the initial state is given by $|\uparrow\rangle_{\mathrm{S}} \prod_n |0\rangle_n := |\uparrow, 0\rangle$. As the interaction Hamiltonian with the RWA preserves excitation number, we thus have, that at any later time the state must be some superposition of $|\uparrow, 0\rangle$ and $|\downarrow, 1_n\rangle := |\downarrow\rangle_{\mathrm{S}} |1\rangle_n \prod_{m\neq n} |0\rangle_m$. This model is exactly solvable using the Wigner–Weisskopf method [73, 74] for $g_n = g =$ constant, which gives

$$c_{\uparrow,0}^{(\mu)} = \frac{g}{\left(g^2 + \frac{\gamma^2}{4} + E_\mu^2\right)^{\frac{1}{2}}}, \quad c_{\downarrow,1_n}^{(\mu)} = \frac{g^2/(E_\mu - \omega_n)}{\left(g^2 + \frac{\gamma^2}{4} + E_\mu^2\right)^{\frac{1}{2}}}, \tag{A5}$$

where $\gamma = \frac{2\pi g^2}{\omega_0}$ is the decay rate. Now, the fluctuations and IPR may be easily calculated for this model in the limit $N \to \infty$. Here we can write $\sum_\mu \to \int \frac{dE_\mu}{\omega_0}$, and as in the continuum limit the level spacing $\omega_0 \to 0$, with $\gamma =$ constant, we have $g^2 = \frac{\gamma\omega_0}{2\pi} \to 0$. We thus have

$$\mathrm{IPR}\left(|\psi(0)\rangle\right) = \frac{\gamma^2\omega_0}{4\pi^2} \int \frac{dE_\mu}{\omega_0} \frac{1}{\left(\frac{\gamma^2}{4} + E_\mu^2\right)^2} = \frac{\omega_0}{\pi\gamma}. \tag{A6}$$

Now, the fluctuations can be found from equation (5). We pick as our observable σ_z, for which we have $(\sigma_z)_{\mu\nu} = c_{\uparrow,0}^{(\mu)} c_{\uparrow,0}^{(\nu)} - \sum_n c_{\downarrow,1_n}^{(\mu)} c_{\downarrow,1_n}^{(\nu)} = 2c_{\uparrow,0}^{(\mu)} c_{\uparrow,0}^{(\nu)} - \delta_{\mu\nu}$. Thus, equation (5) may be similarly evaluated to obtain

$$\delta_{\sigma_z}^2(\infty) = 4\frac{\omega_0^2}{\pi^2\gamma^2} - 10\frac{\omega_0^3}{\pi^3\gamma^3} \approx 4\mathrm{IPR}\left(|\psi(0)\rangle\right)^2. \tag{A7}$$

In figure 5 we plot the DE fluctuations against the IPR for the case where g_n is given by a random number of mean zero and variance g, observing that the obtained scaling is still correct for the non-integrable case with random couplings. In figure 6 we plot the time dependence and long-time average of $F(t)$, for constant couplings $g_n = g$.

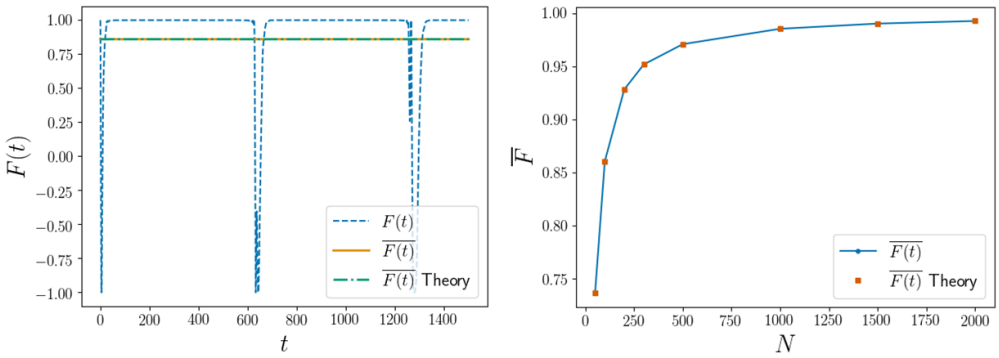

Figure 6. $F(t)$ for $N = 100$ (left) and $\overline{F(t)}$ (right) for the spin-boson Hamiltonian, equation (A1). Theory labels the correlated quench condition result of equation (30). Note that 'revivals' in $F(t)$ significantly contribute to the time average result. $\omega_z = 0.6$, $\omega_n = \frac{n}{N}, \Gamma = \frac{2\pi g^2}{\omega_0} = 0.2$.

We further note that this case is also exactly fulfilled by the tight-binding model, which may be similarly solved by the Wigner–Weisskopf approach.

Appendix B. Time average of *F*(*t*)

Here we calculate the long-time average of $F(t)$, given by

$$\begin{aligned}\overline{F} &= \overline{\langle\uparrow, k_0|W^\dagger(t)V^\dagger W(t)V|\uparrow, k_0\rangle} \\ &= \sum_{\mu\nu} c_\mu(k_0,\uparrow)c_\nu(k_0,\uparrow)\overline{\langle\psi_\mu|W^\dagger(t)V^\dagger W(t)V|\psi_\nu\rangle}.\end{aligned} \tag{B1}$$

We first obtain $\overline{F}_{\mu\nu} := \overline{\langle\psi_\mu|W^\dagger(t)V^\dagger W(t)V|\psi_\nu\rangle}$, which can be seen to be equal to

$$\begin{aligned}\overline{F}_{\mu_0\nu_0} &= \sum_\mu W_{\mu_0\mu_0}V_{\mu_0\mu}W_{\mu\mu}V_{\mu\nu_0} + \sum_\mu W_{\mu_0\mu}V_{\mu\mu}W_{\mu\mu_0}V_{\mu_0\nu_0} \\ &\quad - W^2_{\mu_0\mu_0}V_{\mu_0\mu_0}V_{\mu_0\nu_0} \\ &:= \overline{F}^{(1)}_{\mu_0\nu_0} + \overline{F}^{(2)}_{\mu_0\nu_0} - \overline{F}^{(3)}_{\mu_0\nu_0}\end{aligned} \tag{B2}$$

Now, using that $O_{\mu\nu} = \Delta O c_\mu(\uparrow, k_0)c_\nu(\uparrow, k_0) + O_\downarrow\delta_{\mu\nu}$, we may write, using the shorthand $c_\mu(\uparrow, k_0) := c_\mu$,

$$\begin{aligned}\overline{F}^{(1)}_{\mu_0\nu_0} &= \sum_\mu (\Delta W c_{\mu_0}c_{\mu_0} + W_\downarrow)(\Delta V c_{\mu_0}c_\mu + V_\downarrow\delta_{\mu\mu_0}) \\ &\quad \times (\Delta W c_\mu c_\mu + W_\downarrow)(\Delta V c_\mu c_{\nu_0} + V_\downarrow\delta_{\mu\nu_0}).\end{aligned} \tag{B3}$$

Performing the expansion in full, we obtain

$$\begin{aligned}\overline{F}^{(1)}_{\mu_0\nu_0} = \sum_{\mu}\Big[& W_\downarrow^2 V_\downarrow^2 \delta_{\mu\mu_0}\delta_{\mu\nu_0} + W_\downarrow^2 \Delta V^2 c_\mu^2 c_{\nu_0} c_{\mu_0} \\ & + \Delta W^2 V_\downarrow^2 c_\mu^2 c_{\mu_0}^2 \delta_{\mu\mu_0}\delta_{\mu\nu_0} + \Delta W^2 \Delta V^2 c_\mu^4 c_{\nu_0} c_{\mu_0}^3 \\ & + \Delta W W_\downarrow \Delta V V_\downarrow \left(c_\mu c_{\mu_0}^3 \delta_{\mu\nu_0} + c_\mu^2 c_{\nu_0}\delta_{\mu\mu_0} + c_\mu^3 c_{\mu_0}\delta_{\mu\nu_0} + c_\mu c_{\nu_0} c_{\mu_0}^2 \delta_{\mu\mu_0}\right) \\ & + \Delta W W_\downarrow \Delta V^2 \left(c_\mu^4 c_{\nu_0} c_{\mu_0} + c_\mu^2 c_{\mu_0}^3 c_{\nu_0}\right) \\ & + \Delta W W_\downarrow V_\downarrow^2 \left(c_\mu^2 \delta_\mu^2 \delta_{\mu\mu_0}\delta_{\mu\nu_0} + c_{\mu_0}^2 \delta_{\mu\mu_0}\delta_{\mu\nu_0}\right) \\ & + \Delta W^2 \Delta V V_\downarrow \left(c_\mu^3 c_{\mu_0}^2 c_{\nu_0}\delta_{\mu\mu_0} + c_\mu^3 c_{\mu_0}^3\right) \\ & + W_\downarrow^2 \Delta V V_\downarrow \left(c_\mu c_{\nu_0}\delta_{\mu\mu_0} + c_\mu c_{\mu_0}\delta_{\mu\nu_0}\right)\Big]\end{aligned} \tag{B4}$$

similarly,

$$\begin{aligned}\overline{F}^{(2)}_{\mu_0\nu_0} &= \sum_{\mu}(\Delta W c_{\mu_0} c_\mu + W_\downarrow \delta_{\mu\mu_0})(\Delta V c_\mu c_\mu + V_\downarrow) \\ &\quad \times (\Delta W c_\mu c_{\mu_0} + W_\downarrow \delta_{\mu\mu_0})(\Delta V c_{\mu_0} c_{\nu_0} + V_\downarrow \delta_{\mu_0\nu_0}) \\ &= \sum_{\mu}\Big[W_\downarrow^2 V_\downarrow^2 \delta_{\mu_0\nu_0}\delta_{\mu\mu_0} + W_\downarrow^2 \Delta V V_\downarrow c_\mu^2 \delta_{\mu_0\nu_0}\delta_{\mu\mu_0} \\ &\qquad + 2\Delta W W_\downarrow V_\downarrow^2 c_\mu c_{\mu_0}\delta_{\mu_0\nu_0}\delta_{\mu\mu_0} \\ &\qquad + 2\Delta W W_\downarrow \Delta V V_\downarrow \left(c_\mu^3 c_{\mu_0}\delta_{\mu_0\nu_0}\delta_{\mu\mu_0} + c_\mu c_{\mu_0}^2 c_{\nu_0}\delta_{\mu\mu_0}\right) \\ &\qquad + W_\downarrow^2 \Delta V V_\downarrow c_{\mu_0} c_{\nu_0}\delta_{\mu\mu_0} + W_\downarrow^2 \Delta V^2 c_{\mu_0} c_{\nu_0}\delta_{\mu\mu_0} \\ &\qquad + \Delta W^2 V_\downarrow^2 c_\mu^2 c_{\mu_0}^2 \delta_{\mu_0\nu_0} + \Delta W^2 \Delta V^2 c_\mu^4 c_{\mu_0}^3 c_{\nu_0} \\ &\qquad + 2\Delta W W_\downarrow \Delta V^2 c_\mu^3 c_{\mu_0}^2 c_{\nu_0}\delta_{\mu\mu_0} \\ &\qquad + \Delta W^2 \Delta V V_\downarrow \left(c_\mu^2 c_{\mu_0}^3 c_{\nu_0} + c_\mu^4 c_{\mu_0}^2 \delta_{\mu_0\nu_0}\right)\Big]\end{aligned} \tag{B5}$$

and,

$$\begin{aligned}\overline{F}^{(3)}_{\mu_0\nu_0} &= (\Delta W c_{\mu_0} c_{\mu_0} + W_\downarrow)(\Delta V c_{\mu_0} c_{\mu_0} + V_\downarrow) \\ &\quad \times (\Delta W c_{\mu_0} c_{\mu_0} + W_\downarrow)(\Delta V c_{\mu_0} c_{\nu_0} + V_\downarrow \delta_{\mu_0\nu_0}) \\ &= W_\downarrow^2 V_\downarrow^2 \delta_{\mu_0\nu_0} + W_\downarrow^2 \Delta V V_\downarrow c_{\mu_0}\delta_{\mu_0\nu_0} \\ &\quad + 2\Delta W W_\downarrow V_\downarrow^2 c_{\mu_0}\delta_{\mu_0\nu_0} + W_\downarrow^2 \Delta V^2 c_{\mu_0}^3 c_{\nu_0} \\ &\quad + 2\Delta W W_\downarrow \Delta V V_\downarrow \left(c_{\mu_0}^3 c_{\nu_0} + c_{\mu_0}^4 \delta_{\mu_0\nu_0}\right) \\ &\quad + \Delta W^2 V_\downarrow^2 c_{\mu_0}^4 \delta_{\mu_0\nu_0} + 2\Delta W W_\downarrow \Delta V^2 c_{\mu_0}^5 c_{\nu_0} \\ &\quad + \Delta W^2 \Delta V V_\downarrow c_{\mu_0}^5 c_{\nu_0} + \Delta W^2 \Delta V V_\downarrow c_{\mu_0}^6 \delta_{\mu_0\nu_0} \\ &\quad + \Delta W^2 \Delta V^2 c_{\mu_0}^7 c_{\nu_0}\Big].\end{aligned} \tag{B6}$$

Now, using that,

$$\overline{F(t)} = \sum_{\mu_0\nu_0} c_{\mu_0} c_{\nu_0} \overline{F}_{\mu_0\nu_0}, \tag{B7}$$

and defining

$$\mathcal{I}_n = \sum_{\mu} c_{\mu}^n, \tag{B8}$$

we thus obtain (noting that $\mathcal{I}_2 = 1$),

$$\begin{aligned}\overline{F(t)} = {} & W_\downarrow^2 V_\downarrow^2 + W_\downarrow^2 \Delta V V_\downarrow + W_\downarrow^2 \Delta V^2 + W_\downarrow^2 \Delta V V_\downarrow \\ & + \mathcal{I}_4 [4\Delta W W_\downarrow \Delta V V_\downarrow + 2\Delta W W_\downarrow V_\downarrow^2 \\ & + 2\Delta W^2 W_\downarrow \Delta V^2 + \Delta W^2 V_\downarrow^2 + \Delta W^2 \Delta V V_\downarrow] \\ & + \mathcal{I}_4^2 [2\Delta W^2 \Delta V V_\downarrow + 2\Delta W^2 \Delta V^2] \\ & - \mathcal{I}_8 [\Delta W^2 \Delta V^2 + \Delta W^2 \Delta V V_\downarrow],\end{aligned} \tag{B9}$$

which is the result shown in the main text. We note that terms in $\mathcal{I}_n$ can be seen as finite size effects, which become negligible as $N \to \infty$. Indeed $\mathcal{I}_4$ is equal to the IPR. For large system sizes, we thus expect,

$$\overline{F(t)} \approx W_\downarrow^2 V_\downarrow^2 + W_\downarrow^2 \Delta V V_\downarrow + W_\downarrow^2 \Delta V^2 + W_\downarrow^2 \Delta V V_\downarrow. \tag{B10}$$

We use the full equation in the numerics, however, as the finite size effects can be seen to be important in the system sizes studied numerically.

Appendix C. Discussion of larger system sizes

In the main text we focused on the case where H_S is a 2×2 Hamiltonian matrix. Here we show that in certain conditions the main arguments similarly follow for larger systems, of Hilbert space dimension $\mathcal{N}_\mathrm{S}$, with eigenstates $\{|s\rangle_\mathrm{S}\}_{s=1,\ldots,\mathcal{N}_S}$. We now write the initial state as $|\psi(0)\rangle = |s_i\rangle_\mathrm{S}|k_0\rangle_\mathrm{B}$, where $|k_0\rangle_\mathrm{B}$ is again a non-degenerate state of some conserved quantity, and $|s_i\rangle_\mathrm{S}$ is the initial (excited) system state.

We can show this simply by deriving equation (23) for an arbitrary size H_S. Indeed, we can do this by following the same approach as the main text, with some additional requirements. Writing instead

$$|\psi_\mu\rangle = \sum_k c_\mu(k, s_i)|s_i\rangle_\mathrm{S}|k\rangle_\mathrm{B} + \sum_{s\neq s_i}^{\mathcal{N}_S} \sum_k c_\mu(k,s)|s\rangle_\mathrm{S}|k\rangle_\mathrm{B}. \tag{C1}$$

Now, once again, if the system observable is diagonal in the non-interacting basis, we have $O_{ss'} := \langle s|O|s'\rangle \sim \delta_{ss'}$, such that

$$\begin{aligned}
O_{\mu\nu} &= \sum_k c_\mu(s_i,k)c_\nu(s_i,k)O_{s_is_i} + \sum_{s\neq s_i}\sum_k c_\mu(s,k)c_\nu(s,k)O_{ss} \\
&= \sum_k c_\mu(s_i,k)c_\nu(s_i,k)O_{s_is_i} + \sum_{s\neq s_i} O_{ss}\langle\psi_\mu|\sum_k |s\rangle_{\mathrm{S}}|k\rangle_{\mathrm{BB}}\langle k|_{\mathrm{S}}\langle s|\psi_\nu\rangle \\
&= \sum_k c_\mu(s_i,k)c_\nu(s_i,k)O_{s_is_i} \\
&\quad + \sum_{s\neq s_i} O_{ss}\langle\psi_\mu|\left(\mathbb{1} - \sum_{s'\neq s}\sum_k |s'\rangle_{\mathrm{S}}|k\rangle_{\mathrm{BB}}\langle k|_{\mathrm{S}}\langle s'|\right)|\psi_\nu\rangle \\
&= c_\mu(s_i,k_0)c_\nu(s_i,k_0)O_{s_is_i} - O_{s_is_i}\delta_{\mu\nu} - \sum_{s\neq s_i} O_{ss}\sum_{s'\neq s}\sum_k c_\mu(s',k)c_\nu(s',k),
\end{aligned} \tag{C2}$$

where we have used that O may be taken as traceless, implying $\sum_{s\neq s_i} O_{ss} = -O_{s_is_i}$. Now, we see the same form is recovered up to a correction given by the last term, and thus this term is dictated by the quantity $\sum_k c_\mu(s,k)c_\nu(s,k)$. Assuming conservation of excitation number, and thus this summation is given by

$$\sum_{s'\neq s}\sum_k c_\mu(s',k)c_\nu(s',k) = \sum_{\Delta s\neq 0} c_\mu(s_0-\Delta s, k_0+\Delta s), \tag{C3}$$

where $\Delta s = s_i - s'$ is the change in excitation number of the system. Note that Δs is always positive when $|k_0\rangle_B$ is initialized with zero excitations, or if the $s_i = \max s$. We then have the correction term as equal to

$$-\sum_{s\neq s_i} O_{ss}\sum_{s'\neq s} c_\mu(s',k_0+s_i-s')c_\nu(s',k_0+s_i-s'). \tag{C4}$$

For high $\mathcal{N}_{\mathrm{S}}$, then, this term can dominate the off-diagonal contribution. We note, however, that for transnationally invariant eigenstates, as expected for a many-body quantum system away from the edges (which we note the total system + bath state fulfils, given that the initial system energy is large enough), we can write $c_\mu(s,k) \approx c_\mu(s+k)$, and thus the correction term becomes,

$$O_{s_is_i}(\mathcal{N}_{\mathrm{S}}-1)c_\mu(k_0,s_i)c_\nu(k_0,s_i), \tag{C5}$$

where we have once again used that O may be taken as traceless. We then have,

$$O_{\mu\nu} \approx O_{s_is_i}\mathcal{N}_{\mathrm{S}}c_\mu(k_0+s)c_\nu(k_0+s) - O_{s_is_i}\delta_{\mu\nu}, \tag{C6}$$

which is of the form of equation (23).

Appendix D. Robustness to multiple excitations

In this section we show that in some cases equation (23) may be applied outside the regime where it is exact, that is, to the case where there is no conservation law that we may use as our excitation number. We will see that when the initial bath state is the ground state of H_{B}, equation (23) is approximately fulfilled due to the energy cost associated to an excited state of the bath.

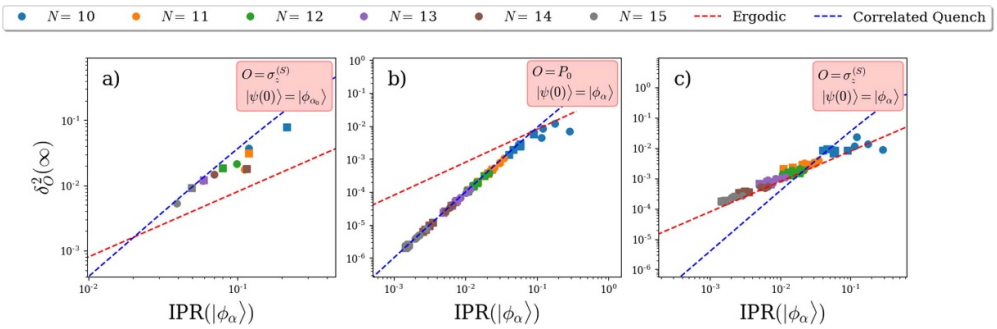

Figure 7. DE Fluctuations versus IPR for Hamiltonian equations (D1)–(D3). $B_x^{(\mathrm{S})} = 0, B_x^{(\mathrm{B})} = 0.3, B_z^{(\mathrm{S})} = 0.8, B_z^{(\mathrm{B})} = 0, J_x^{(\mathrm{B})} = 1, J_z^{(\mathrm{B})} = 0.1$. Coupling strengths: $J_x^{(\mathrm{SB})} = 0.8, 1.0$ for circles and squares respectively. Initial state is $|\uparrow\rangle_{\mathrm{S}}|\psi_{\alpha_0}\rangle_{\mathrm{B}}$, where $|\psi_{\alpha_0}\rangle_{\mathrm{B}}$ is the ground state of the bath Hamiltonian H_{B}. $N_m = 5$, such that the chain is non-integrable.

D.1. Removing excitation conservation

We will observe this using a different spin-chain Hamiltonian, of the form $H = H_{\mathrm{S}} + H_{\mathrm{B}} + H_{\mathrm{SB}}$, with

$$H_{\mathrm{S}} = B_z^{(\mathrm{S})}\sigma_z^{(1)} \tag{D1}$$

where $\{\sigma_i^{(n)}\}$ $i = x, y, z$ are the Pauli operators acting on site n. The bath Hamiltonian is a spin-chain of length N, with nearest-neighbour Ising and XX interactions subjected to both B_z and B_x fields

$$H_{\mathrm{B}} = \sum_{n>1}^{N}\left(B_z^{(\mathrm{B})}\sigma_z^{(n)} + B_x^{(\mathrm{B})}\sigma_x^{(n)} + \sum_{n>1}^{N-1} J_z\sigma_z^{(n)}\sigma_z^{(n+1)} + J_x\left(\sigma_+^{(n)}\sigma_-^{(n+1)} + \sigma_-^{(n)}\sigma_+^{(n+1)}\right)\right). \tag{D2}$$

The interaction part of the Hamiltonian is given by,

$$H_{\mathrm{SB}} = J_x^{(\mathrm{SB})}\left(\sigma_+^{(1)}\sigma_-^{N_m} + \sigma_-^{(1)}\sigma_+^{N_m}\right), \tag{D3}$$

where we use $N_m = 5$ throughout, such that the bath is described by a 1-D chain with indices $2, \ldots, N$, and the system (site 1) is coupled to a single spin at site 5.

In this case, we have that there is no conservation of excitation number, so equation (23) is at best approximate. In figure 7 we plot the scaling of fluctuations for this Hamiltonian for two initial states. In the first, we have the system initialized in the excited state $|\uparrow\rangle_{\mathrm{S}}$, and the bath initialized in the ground state of H_{B}, and for the second, we choose the same system state, and a random mid-energy eigenstate of the bath. We observe that for the bath ground state initial state, figure 7(a), the correlated quench results are still a good approximation, however this gets worse as the systems size increases, due to the presence of more states lying are close to

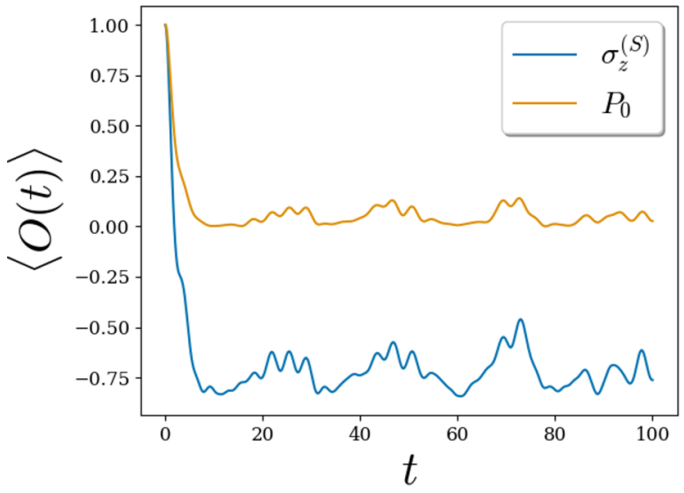

Figure 8. Dynamics of observable $\sigma_z^{(\mathrm{S})}$ (blue) and P_0 (orange) for Hamiltonian equations (D1)–(D3). $B_x^{(\mathrm{S})} = 0, B_x^{(\mathrm{B})} = 0.3, B_z^{(\mathrm{S})} = 0.8, B_z^{(\mathrm{B})} = 0, J_x^{(\mathrm{B})} = 1, J_z^{(\mathrm{B})} = 0.1$. Coupling strengths: $J_x^{(\mathrm{SB})} = 0.8, 1.0$ for circles and squares respectively. Initial state is $|\uparrow\rangle_{\mathrm{S}}|\psi_{\alpha_0}\rangle_{\mathrm{B}}$, where $|\psi_{\alpha_0}\rangle_{\mathrm{B}}$ is the ground state of the bath Hamiltonian H_{B}. $N_m = 5, N = 14$.

the ground state with multiple excitations, that are able to be excited. As above, we see the fluctuations in survival probability differ from the ETH prediction, figure 7(b), for all initial states, and the random mid-energy eigenstates scale according to the ETH, figure 7(c).

We thus observe the implied scaling is robust in some cases to the presence of non-excitation number conserving terms. This can be attributed to a similar mechanism, where due to conservation of energy, if the system is measured to be in the excited state, the bath is (at least likely to be) in the ground state, and thus the system observable is equivalent to the survival probability. This can be seen in the case of time evolution, see figure 8, where we see the description of diagonal local systems observables in terms of the survival probability remains a good approximation.

D.2. Excited initial bath states

In this section we present numerics showing the robustness of the correlated quench results to initial states that have multiple excitations. For this, we use the Hamiltonian of equation (D2) of the main text, and report initial product states of multiple excitations.

In figure 9 we see that the scaling of fluctuation implied by the correlated quench is valid for initial states that are low-lying excited states of the bath, rather than only for a zero excitation initial bath state. This effect, however, is far more sensitive to initial excitations than to symmetry breaking terms in the bath Hamiltonian, as the Hilbert space dimension of higher manifolds grows quickly with the number of excitations for a small excitation number. We observe a crossover to the ETH scaling for excited bath states as N is increased.

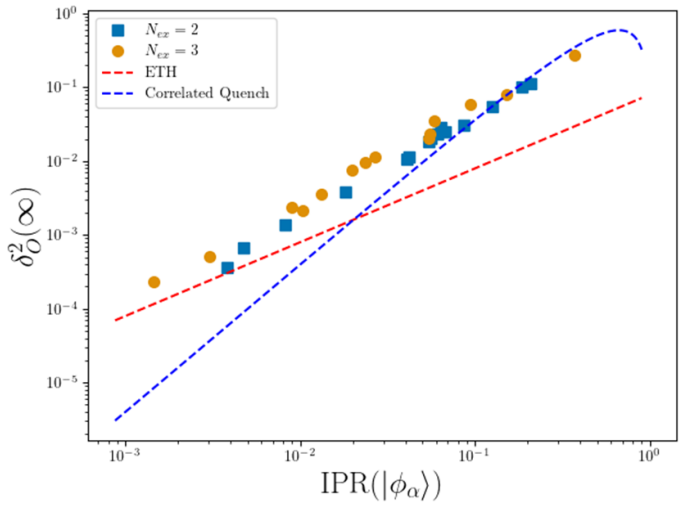

Figure 9. Scaling of observable fluctuations with number of spins N for initial states with small number of excitations in the bath. We show an average over 200 different initial states where N_{ex} random spins of the bath are excited. N increases to the left and takes values [5–15, 2, 30, 40, 5] and [3–15, 20, 25] for $N_{\mathrm{ex}} = 2$ and 4, respectively.

ORCID iDs

Charlie Nation https://orcid.org/0000-0002-3770-8980
Diego Porras https://orcid.org/0000-0003-2995-0299

References

[1] Rigol M, Dunjko V and Olshanii M 2008 *Nature* **452** 854–8
[2] Yukalov V 2011 *Laser Phys. Lett.* **8** 485–507
[3] Eisert J, Friesdorf M and Gogolin C 2014 *Nat. Phys.* **11** 124–30
[4] D'Alessio L, Kafri Y, Polkovnikov A and Rigol M 2016 *Adv. Phys.* **65** 239–362
[5] Gogolin C and Eisert J 2016 *Rep. Prog. Phys.* **79** 056001
[6] Borgonovi F, Izrailev F M, Santos L F and Zelevinsky V G 2016 *Phys. Rep.* **626** 1–58
[7] Mori T, Ikeda T N, Kaminishi E and Ueda M 2018 *J. Phys. B: At. Mol. Phys.* **51** 112001
[8] Ueda M 2020 *Nat. Rev. Phys.* **2** 669–81
[9] Gring M, Kuhnert M, Langen T, Kitagawa T, Rauer B, Schreitl M, Mazets I, Adu Smith D, Demler E and Schmiedmayer J 2012 *Science* **337** 1318–22
[10] Schneider C, Porras D and Schaetz T 2012 *Rep. Prog. Phys.* **75** 24401–33
[11] Georgescu I M, Ashhab S and Nori F 2014 *Rev. Mod. Phys.* **86** 153–85
[12] Schreiber M, Hodgman S S, Bordia P, Lüschen H P, Fischer M H, Vosk R, Altman E, Schneider U and Bloch I 2015 *Science* **349** 842–5
[13] Neill C *et al* 2016 *Nat. Phys.* **12** 1037–41
[14] Kaufman A M, Eric Tai M, Lukin A, Rispoli M, Schittko R, Preiss P M and Greiner M 2016 *Science* **353** 790–4
[15] Clos G, Porras D, Warring U and Schaetz T 2016 *Phys. Rev. Lett.* **117** 170401
[16] Deutsch J M 1991 *Phys. Rev.* A **43** 2046–9
[17] Srednicki M 1996 *J. Phys. A: Math. Gen.* **29** 75–79
[18] Kim H, Ikeda T N and Huse D A 2014 *Phys. Rev.* E **90** 052105
[19] Mondaini R, Fratus K R, Srednicki M and Rigol M 2016 *Phys. Rev.* E **93** 032104
[20] Mondaini R and Rigol M 2017 *Phys. Rev.* E **96** 012157
[21] Reimann P 2015 *New J. Phys.* **17** 055025

[22] Nation C and Porras D 2018 *New J. Phys.* **20** 103003
[23] Dabelow L and Reimann P 2020 *Phys. Rev. Lett.* **124** 120602
[24] Nation C and Porras D 2019 *Phys. Rev.* E **99** 052139
[25] Reimann P and Dabelow L 2021 *Phys. Rev.* E **103** 022119
[26] Srednicki M 1999 *J. Phys. A: Math. Gen.* **32** 1163–75
[27] Reimann P 2008 *Phys. Rev. Lett.* **101** 190403
[28] Cassidy A C, Clark C W and Rigol M 2011 *Phys. Rev. Lett.* **106** 140405
[29] Malabarba A S L, Garcia-Pintos L P, Linden N, Farrelly T C and Short A J 2014 *Phys. Rev.* E **90** 012121
[30] García-Pintos L P, Linden N, Malabarba A S L, Short A J and Winter A 2017 *Phys. Rev.* X **7** 031027
[31] Reimann P 2016 *Nat. Commun.* **7** 10821
[32] Borgonovi F, Izrailev F M and Santos L F 2019 *Phys. Rev.* E **99** 010101(R)
[33] Alhambra A M, Riddell J and García-Pintos L P 2020 *Phys. Rev. Lett.* **124** 110605
[34] Shiraishi N and Mori T 2017 *Phys. Rev. Lett.* **119** 030601
[35] Mondaini R, Mallayya K, Santos L F and Rigol M 2018 *Phys. Rev. Lett.* **121** 038901
[36] Moudgalya S, Bernevig B A and Regnault N 2021 arXiv:2109.00548
[37] Serbyn M, Abanin D A and Papić Z 2021 *Nat. Phys.* **17** 675–85
[38] Bernien H *et al* 2017 *Nature* **551** 579–84
[39] Buča B, Tindall J and Jaksch D 2019 *Nat. Commun.* **10** 1730
[40] Dağ C B, Sun K and Duan L M 2019 *Phys. Rev. Lett.* **123** 140602
[41] Flambaum V V and Izrailev F M 1997 *Phys. Rev.* E **56** 5144–59
[42] Torres-Herrera E J, Karp J, Tavora M and Santos L F 2016 *Entropy* **18** 359
[43] Nickelsen D and Kastner M 2019 arXiv:1912.02043
[44] Nation C and Porras D 2020 *Phys. Rev.* E **102** 042115
[45] Neumann J V 2010 *Eur. Phys. J.* H **237** 41
[46] Goldstein S, Lebowitz J L, Mastrodonato C, Tumulka R and Zangh N 2009 arXiv:0911.1724
[47] Vidmar L and Rigol M 2016 *J. Stat. Mech.* 064007
[48] Nation C and Porras D 2019 *Quantum* **3** 207
[49] Borgonovi F, Mattiotti F and Izrailev F M 2017 *Phys. Rev.* E **95** 042135
[50] Short A J 2011 *New J. Phys.* **13** 053009
[51] Borgonovi F and Izrailev F M 2019 *Phys. Rev.* E **99** 012115
[52] Pietracaprina F, Gogolin C and Goold J 2017 *Phys. Rev.* B **95** 125118
[53] Goldstein S, Lebowitz J L, Tumulka R and Zanghì N 2006 *Phys. Rev. Lett.* **96** 050403
[54] Reimann P 2007 *Phys. Rev. Lett.* **99** 160404
[55] Popescu S, Short A J and Winter A 2006 *Nat. Phys.* **2** 754–8
[56] Kubo R 1966 *Rep. Prog. Phys.* **29** 255
[57] Breuer H P and Petruccione F 2002 *The Theory of Open Quantum Systems* (Oxford: Oxford University Press)
[58] Venuti L C and Liu L 2019 arXiv:1904.02336
[59] Maldacena J, Shenker S H and Stanford D 2016 *J. High Energy Phys.* JHEP08(2016)106
[60] Hashimoto K, Murata K and Yoshii R 2017 *J. High Energy Phys.* JHEP10(2017)138
[61] Yan B, Cincio L and Zurek W H 2020 *Phys. Rev. Lett.* **124** 160603
[62] Swingle B 2018 *Nat. Phys.* **14** 988–90
[63] Iyoda E and Sagawa T 2018 *Phys. Rev.* A **97** 042330
[64] Huang Y, Brandão F G S L and Zhang Y L 2019 *Phys. Rev. Lett.* **123** 010601
[65] Foini L and Kurchan J 2019 *Phys. Rev.* E **99** 042139
[66] Murthy C and Srednicki M 2019 *Phys. Rev. Lett.* **123** 230606
[67] Roberts D A and Yoshida B 2017 *J. High Energy Phys.* JHEP04(2017)121
[68] Dağ C B, Duan L M and Sun K 2020 *Phys. Rev.* B **101** 104415
[69] Chan A, De Luca A and Chalker J T 2019 *Phys. Rev. Lett.* **122** 220601
[70] Schiulaz M, Torres-Herrera E J, Pérez-Bernal F and Santos L F 2020 *Phys. Rev.* B **101** 174312
[71] Reimann P 2019 *New J. Phys.* **21** 053014
[72] He K and Rigol M 2013 *Phys. Rev.* A **87** 043615
[73] Weisskopf V and Wigner E 1930 *Z. Phys.* **63** 54–73
[74] Cohen-Tannoudji C, Dupont-Roc J and Grynberg G 1998 *Atom-Photon Interactions: Basic Processes and Applications* (New York: Wiley) p 678